Supplementary Information (SI) for RSC Advances.

Supplementary Information

Roles of Surface Functionalization on the Electrosynthesis of Molecularly Imprinted Polymers (MIPs) and the Detection of Per- and Polyfluoroalkyl Substances (PFAS)

Daniel A. Bellido-Aguilar, McKenna Dunmyer, Cameron S. Malloy, Matthew J. Danley,
Vasiliki Karanikola, Suchol Savagatrup*

Department of Chemical and Environmental Engineering, the University of Arizona, 1133 E. James E. Rogers Way, Tucson Arizona 85721

*Author to whom correspondence should be addressed: S.S. (suchol@arizona.edu)

1. Materials

Perfluorooctane sulfonic acid (PFOS) solution (40% in H_2O), L-cysteine (97%), 1-octanethiol (98.5%), and ferrocene carboxylic acid (97%) were obtained from Millipore Sigma. Ortho-Phenylenediamine (o-PD, 98%) was purchased from Thermo Scientific Chemicals.

2. Au electrodes preparation

Au electrodes were prepared on glass substrates by using an E-Beam PVD equipment (BOC Edwards Auto 306) with a thickness of 100 nm with 10 nm of Cr as the adhesive layer.

3. Au electrode modification

a) Cleaning treatment. The gold electrodes were cleaned by bath sonication in detergent solution for 30 minutes, followed by rinsing with DI water, drying with a stream of compressed air, and 10 minutes of UV/Ozone treatment.

b) Functionalization. The gold electrodes were also modified by surface functionalization. Two different thiol compounds with polar and non-polar chains were employed: L-cysteine (Cys) and 1-octanethiol (OT). The clean Au electrodes were functionalized by soaking them into a 10mM thiol solution for 24 hours. The Cys solution was prepared in DI water and OT solution was prepared in pure ethanol. After soaking, the electrodes were then gently rinsed with DI water and ultrasonicated in either DI water or ethanol for 10 minutes each.

4. Polymer coating synthesis

The electropolymerization of o-PD was performed on the Au electrodes based on the report of Karimian et al.[20] with a few modifications. The MIP synthesis was performed in a three-electrode electrochemical cell where the modified Au electrode, a Pt sheet electrode, and a Ag/AgCl electrode acted as the working, counter, and reference electrodes, respectively. For the synthesis of MIP, the molar ratio between o-PD and PFOS was adjusted so that 10 mM o-PD and 0.05 mM PFOS were prepared in a 2:1 (v:v) acetate buffer (pH = 5.8) to methanol solution. The solution was mixed for 1 h prior to synthesis. The synthesis was carried out by cyclic voltammetry of 25 scans from 0.0 to 1.0 V vs Ag/AgCl at 50 mV s^{-1}. Subsequently, the removal of the template molecules from the coatings was done by a solvent treatment, which consisted of soaking in methanol for 15 s, followed by soaking for 20 min in a water/methanol solution (1:1, v:v) under mild stirring, and finally soaking under methanol for 30 s. Coatings prepared on Au-OT and Au-Cys were denoted as MIP-OT and MIP-Cys, respectively. The synthesis of the non-molecularly imprinting polymer (NIP) was performed in the same manner as in MIP without PFOS. After synthesis, NIP coatings underwent the same solvent treatment as MIP samples.

5. Characterization

Elemental analysis was carried out by X-ray Photoelectron Spectroscopy (XPS) using a Kratos Axis Ultra X-ray photoelectron spectrometer with a pass energy of 20 eV. The x-ray source was Al Kα operated at 15 kV and 20 mA. Water contact angles measurements were performed in a goniometer (Kruss Scientific DSA25E) with 5 µL DI water droplets. The thicknesses of the polymer films were measured using a profilometer (KLA-Tencor 15) with at least 7 measurements for each sample. An Atomic Force Microscope (AFM, Park NX20) L

The sensing properties of the MIP coatings towards PFOS were evaluated electrochemically by assessing the redox reaction of ferrocenecarboxylic acid. The experiments were carried out in a 0.5 mM ferrocene carboxylic acid (FcCOOH) solution in 0.01 M ammonia buffer (pH = 8.4) containing various concentrations of PFOS. The MIP electrode was allowed to interact with the PFOS for 15 minutes before the electrochemical test. Cyclic voltammetry of 20 scans was performed from 0 to 0.50 V Ag/AgCl at 50 mV/s. The average of the 20 scans was taken for analysis where the value of oxidation peak was recorded.

Quartz-crystal microbalance with dissipation (QCM-D) experiments were carried out by using a Q-Sense Explorer (Biolin Scientific) on bare Au and functionalized Au sensors. The cleaning and functionalization of the Au sensors were done identically as in the preparation of MIP coatings. An aqueous solution of PFOS (0.05 mM) was fed into the cells at a constant flow rate (300 μL min^{-1}) until equilibrium was reached. DI water was used as blank before the injection of PFOS solution.

Table S1. Atomic concentration percentages of elements detected by XPS. The abbreviations NTR and TR stand for no template removal and template removal, respectively.

		Au	C	O	N	F	S (thiol)	S(sulfonic)
Au		63.94	25.84	10.22				
Au-Cys		61.83	25.01	8.48	2.81		1.87	
Au-OT		63.42	33.82				2.76	
NIP-Au	(NTR)	0.94	75.94	2.25	20.87			
	(TR)	6.77	71.01	5.09	17.13			
NIP-Cys	(NTR)	0.77	76.25	4.40	18.24			0.35
	(TR)	6.72	72.54	5.52	15.22			
NIP-OT	(NTR)	1.84	73.29	4.45	20.41			
	(TR)	9.01	69.79	4.91	15.79			0.49
MIP-Au	(NTR)	0.80	65.92	3.26	16.36	12.79		0.86
	(TR)	12.18	67.65	4.49	15.68			
MIP-Cys	(NTR)	0.61	68.53	3.94	14.98	11.25		0.69
	(TR)	8.62	71.58	4.67	15.13			
MIP-OT	(NTR)	0.23	67.18	3.44	15.00	13.36		0.78
	(TR)	5.79	74.58	5.47	14.16			

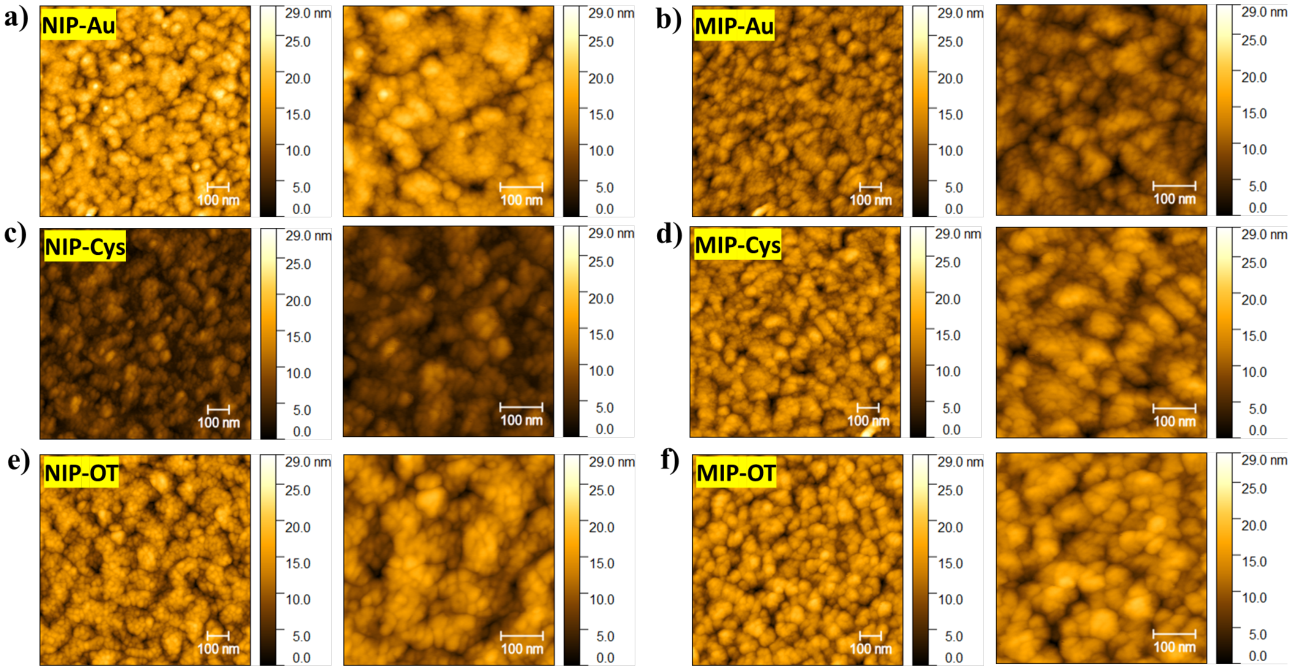

Figure S1. Atomic force microscopy (AFM) images at two magnifications of coatings after template removal for (a) NIP on bare gold (NIP-Au), (b) MIP on bare gold (MIP-Au), (c) NIP on L-cysteine functionalized gold (NIP-Cys), (d) MIP on L-cysteine functionalized gold (MIP-Cys), (e) NIP on 1-octanethiol functionalized gold (NIP-OT), and (f) MIP on 1-octanethiol functionalized gold (MIP-OT).

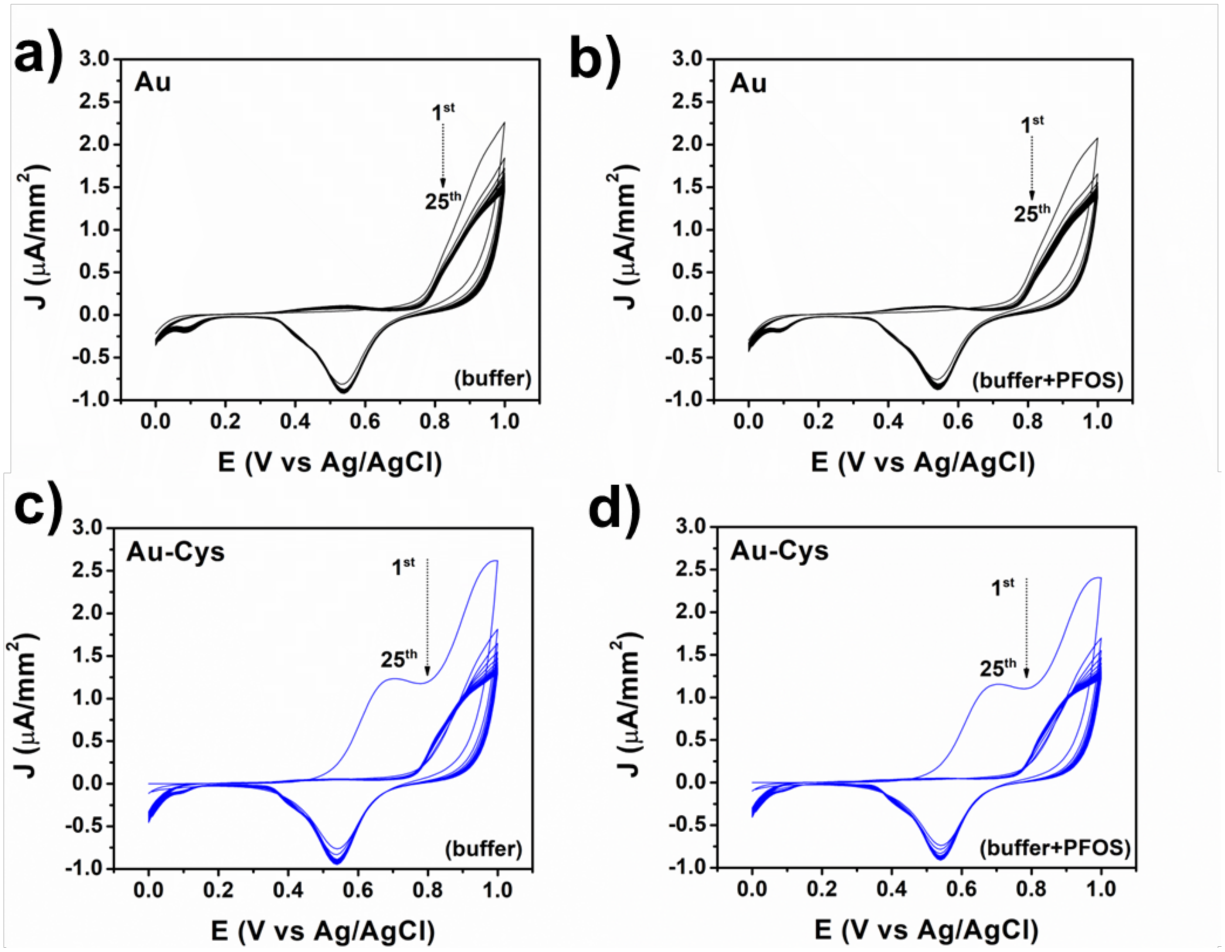

Figure S2. Representative CV curves (25 scans) of different electrodes in the synthesis solution without and with PFOS: (a) bare gold electrode without PFOS, (b) bare gold electrode with PFOS, (c) L-cysteine functionalized gold without PFOS, (d) L-cysteine functionalized gold with PFOS, (e) 1-octanethiol functionalized gold without PFOS, and (f) 1-octanethiol functionalized gold with PFOS. (g) and (h) show the CV curves of 1-octanethiol functionalized gold (Au-OT) without and with PFOS, respectively, in an extended potential range. The arrows indicate the sequence of CV scans.

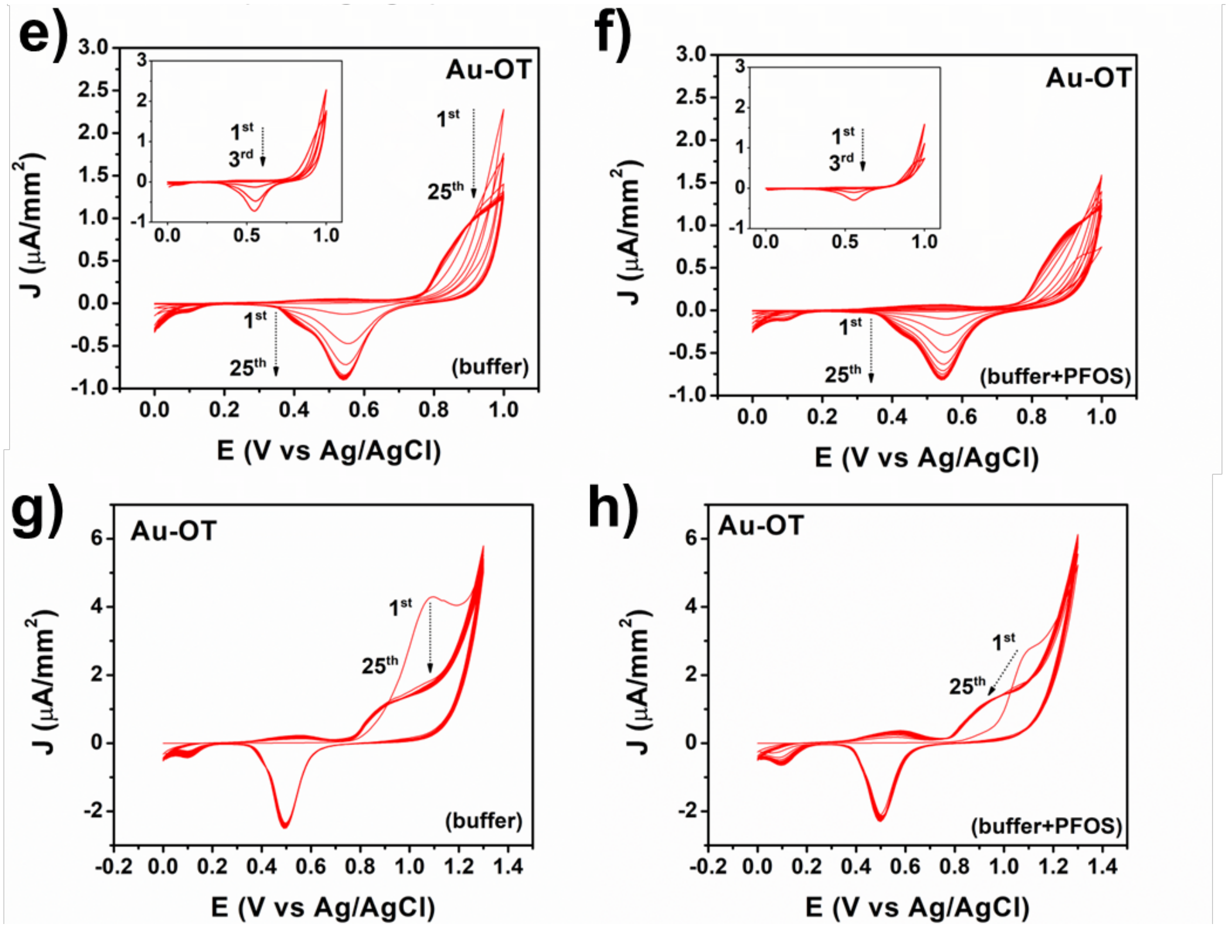

Figure S2 (cont.). Representative CV curves (25 scans) of different electrodes in the synthesis solution without and with PFOS: (a) bare gold electrode without PFOS, (b) bare gold electrode with PFOS, (c) L-cysteine functionalized gold without PFOS, (d) L-cysteine functionalized gold with PFOS, (e) 1-octanethiol functionalized gold without PFOS, and (f) 1-octanethiol functionalized gold with PFOS. (g) and (h) show the CV curves of 1-octanethiol functionalized gold (Au-OT) without and with PFOS, respectively, in an extended potential range. The arrows indicate the sequence of CV scans.

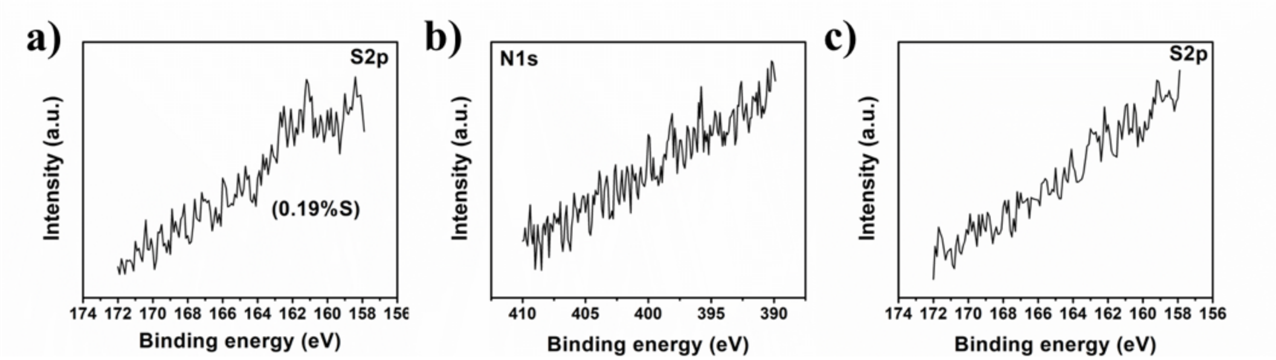

Figure S3. (a) XPS S 2p spectrum and (b) N 1s spectrum of L-cysteine functionalized gold (Au-Cys) tested after cyclic voltammetry tests in the buffer solution without PFOS. (c) XPS S 2p spectrum of Au-OT tested after cyclic voltammetry.

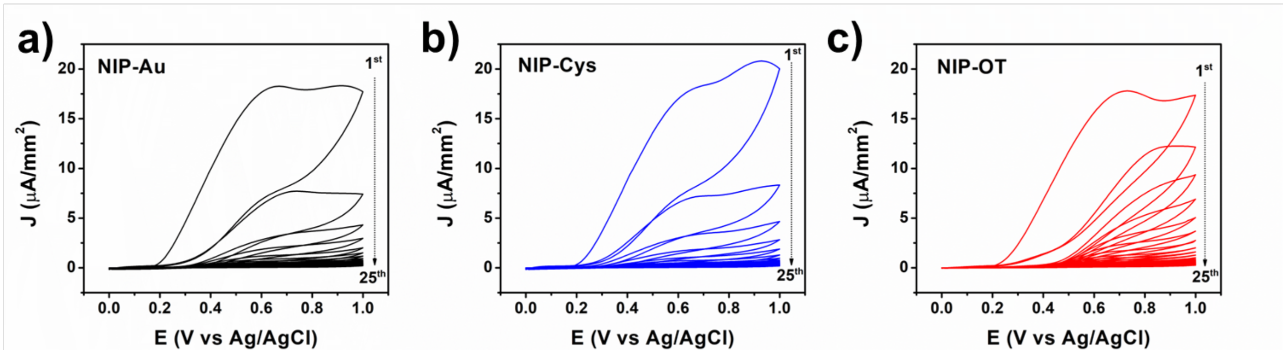

Figure S4. Representative CV curves (25 scans) of the synthesis of the NIP samples (a) on bare gold electrode (NIP-Au), (b) on L-cysteine functionalized gold (NIP-Cys), and (c) on 1-octanethiol functionalized gold (NIP-OT). The arrows indicate the sequence of CV scans.

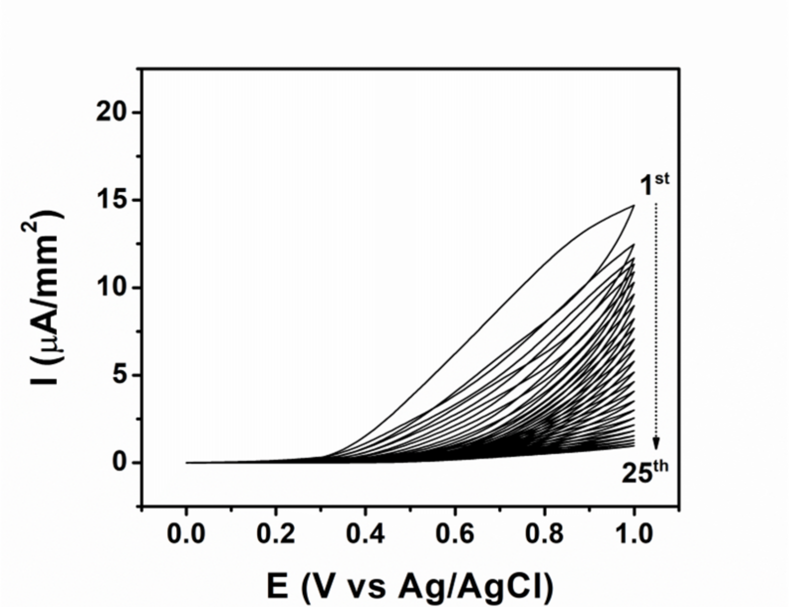

Figure S5. Cyclic voltammogram of NIP synthesis on a gold electrode functionalized with 1-dodecanethiol. The functionalization of gold and NIP synthesis was also carried out as in the other samples.

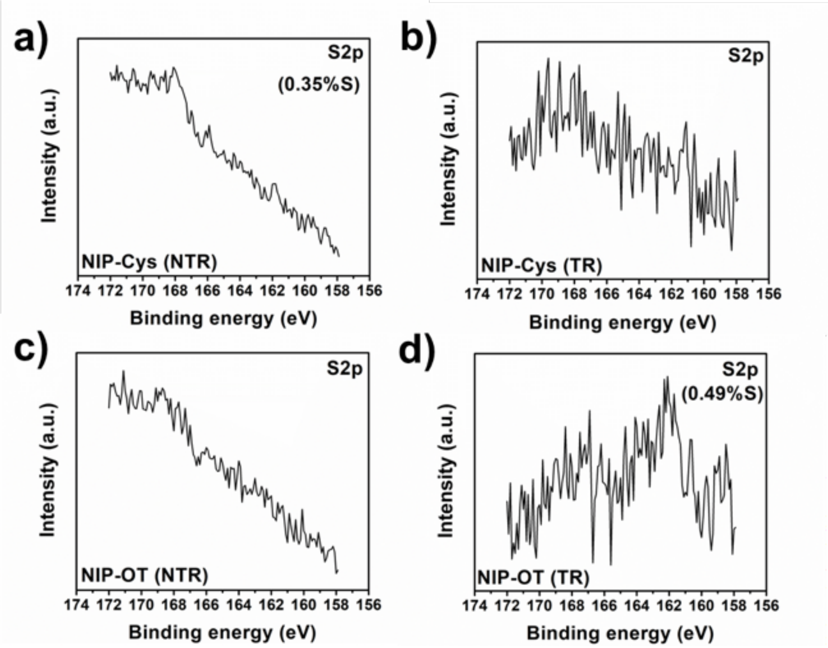

Figure S6. XPS S2p peaks of NIP-Cys (a-b) and NIP-OT (c-d) with no template removal (NTR) and with template removal (TR) step, respectively. The atomic sulfur percentages are shown in the plots.

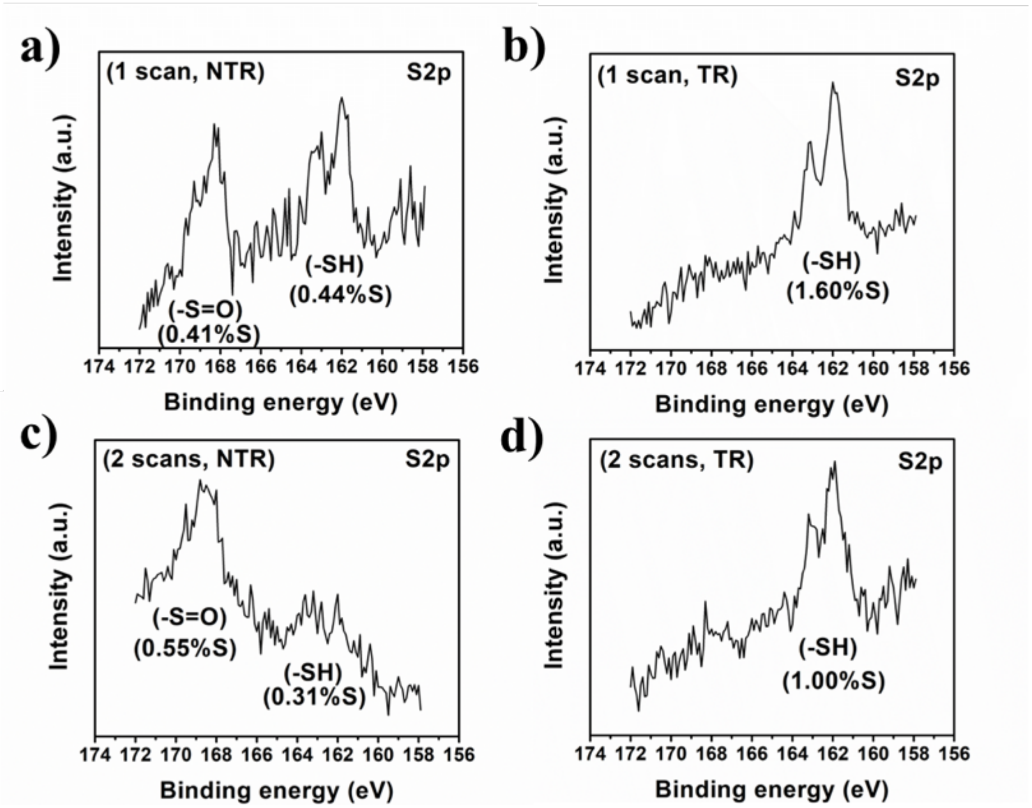

Figure S7. XPS atomic sulfur percentages of MIP-OT after one (a and b) and two (c and d) synthesis scans. The analyses were done with no template removal (NTR) and with template removal (TR) steps. The thicknesses of the coatings were (a) 128 ± 40 nm, (b) 72 ± 36 nm, (c) 208 ± 48 nm, and (d) 73 ± 20 nm.

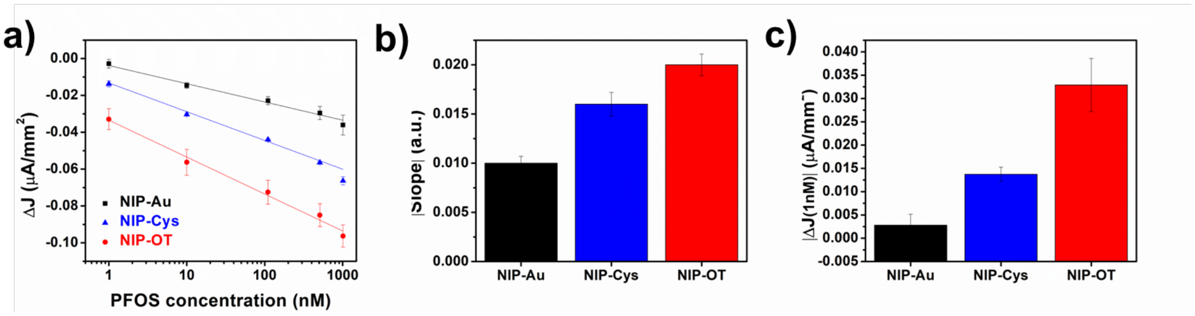

Figure S8. (a) Calibration curves of NIP samples on bare gold electrode (NIP-Au), L-cysteine functionalized gold (NIP-Cys), and 1-octanethiol functionalized gold (NIP-OT) with linear fittings curves. (b) Absolute values of the slope of the linear fittings. (c) Absolute *ΔJ* values at 1 nM PFOS. The slope values of the linear fittings of NIPs (**Figure S8b**) and their *ΔJ* (at 1 nM PFOS) values (**Figure S8c**) showed that the sensitivity decreased as NIP-OT > NIP-Cys > NIP-Au. Interestingly, this trend agreed with the trend observed in MIP samples, suggesting that the hydrophobic functionalization favors the PFOS sensitivity over the hydrophilic functionalization.

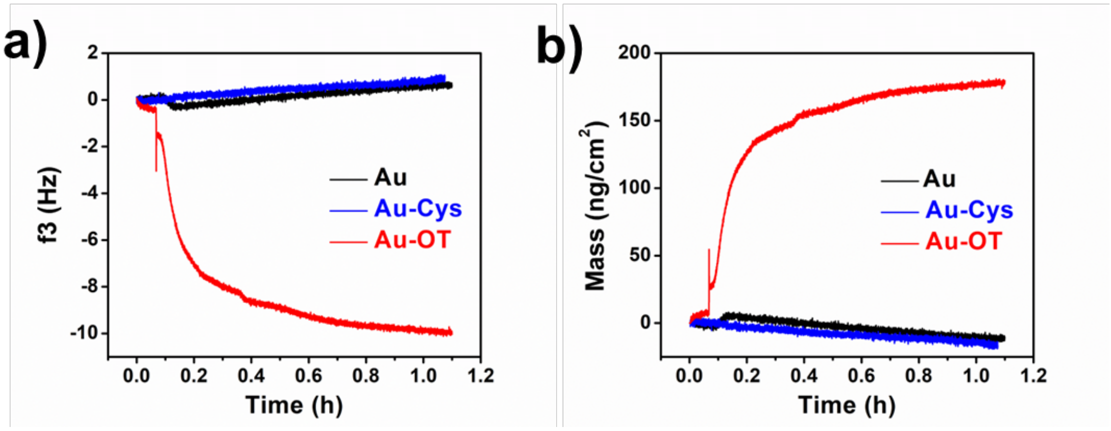

Figure S9. (a) QCM-D frequency (third overtone) profiles of PFOS absorption on the bare sensor (Au), on cysteine-functionalized sensor (Au-Cys) and 1-octanethiol-functionalized sensor (Au-OT). (b) PFOS mass adsorption profiles of the functionalized sensors obtained by the Sauerbrey equation.